

## Self-Supported Organometallic Rhodium Quinonoid Nanocatalysts for Stereoselective Polymerization of Phenylacetylene

Kang Hyun Park,<sup>†</sup> Kwonho Jang,<sup>†</sup> Seung Uk Son,<sup>\*,†</sup> and Dwight A. Sweigart<sup>\*,‡</sup>

Department of Chemistry, Sungkyunkwan University, Suwon 440-746, Korea, and Department of Chemistry, Brown University, Providence, Rhode Island 02912

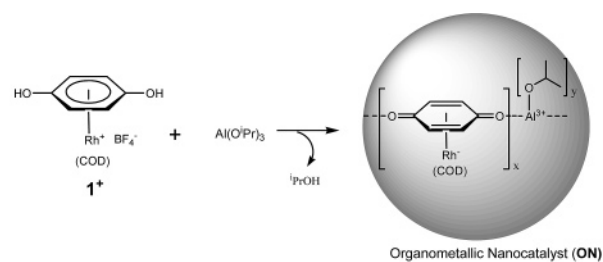
Received April 26, 2006; E-mail: sson@skku.edu

Two important properties that influence the activity and the ease of product separation of heterogeneously catalyzed reactions are the physical size and the size distribution of the catalyst. This is particularly true of nanosized heterogeneous catalysts, which hold much promise for the unprecedented control of reactivity and stereoselectivity in chemical transformations.<sup>1</sup>

A number of methods have been developed for the heterogenization or immobilization of homogeneous catalysts. These include common grafting of the catalyst to solid supports and the use of ionic liquid–organic solvent multiphasic media.<sup>2,3</sup> Another recent and promising approach involves heterogenization of the catalyst or a precursor by ligand modification to generate a self-supporting insoluble polymeric network architecture akin to that used to synthesize metal–organic coordination networks.<sup>4</sup> In comparison to other methods, the self-supporting methodology can produce heterogeneous catalysts during the immobilization process with an unusually high density of catalytically active units.

Many homogeneous organometallic catalysts are known,<sup>5</sup> and the synthesis of nano- and microsized colloidal coordination networks has been described.<sup>6</sup> Herein, we report the first nanosized self-supported *organometallic* catalyst and demonstrate its high activity in the stereoselective polymerization of phenylacetylene. We recently reported the synthesis, self-assembly, and deprotonation of  $[(\eta^6\text{-}1,4\text{-hydroquinone})\text{Rh}(\text{COD})]^+(\text{I}^+)$ , as well as the multifunctional catalytic behavior of  $\text{I}^-$ , in the arylation of benzaldehydes with boronic acids.<sup>7</sup>

Treatment of  $\text{I}^+$  with 1 equiv  $\text{Al}(\text{O}i\text{-Pr})_3$  in 23 mL of THF afforded an insoluble yellow solid and 2-propanol (Figure 1). Figure 2a shows the field emission scanning microscopy (FE-SEM) image of the 340-nm sized organometallic nanocatalyst (**ON3**). Reduction in the reaction volume produced an increase in the average particle size: **ON2** = 402 nm; **ON1** = 537 nm (see Figure S1 in the Supporting Information for size distributions). The yellow **ON** precipitates were formed immediately after addition of the  $\text{Al}(\text{O}i\text{-Pr})_3$  solution, indicating that the size increase with reduced solvent volume is due to an increased growth rate rather than an increase in the number of nuclei formed. Energy dispersive spectroscopy analysis of the synthesized solids using FE-SEM showed that **ON1–3** contain Rh and Al in about 38 to 62 mol % ratio. When 2 equiv of  $\text{Al}(\text{O}i\text{-Pr})_3$  was used, the portion of Rh was slightly decreased to 35 mol %. From inductively coupled plasma atomic emission spectroscopy, the absolute quantity of rhodium in **ON1–3** was determined as 30 wt %. The X-ray photoelectron spectroscopy (XPS) spectrum<sup>8</sup> of **ON3** (Figure 2b) has two Rh 3d orbital peaks at 308 and 313 eV. The Al 2p orbital peak appeared at 75.4 eV, which implies an Al(III) species (see Supporting Information). The solid-state <sup>27</sup>Al NMR spectrum (Figure 2c) indicates hexa-coordination at the Al, possibly indicating aggregation via  $\mu_2\text{-O}$  bonding.<sup>9</sup>



Catalyst	Sol.(mL)	Al(O <sup><i>i</i></sup> -Pr) <sub>3</sub>	Rh:Al	Size(nm)	S.D.(%)
<b>ON1</b>	5.5	1eq	38:62	537	19
<b>ON2</b>	13	1eq	39:61	402	23
<b>ON2-Al</b>	13	2eq	35:65	399	21
<b>ON3</b>	23	1eq	38:62	340	21

Figure 1. Synthesis of self-supported organometallic nanocatalyst.

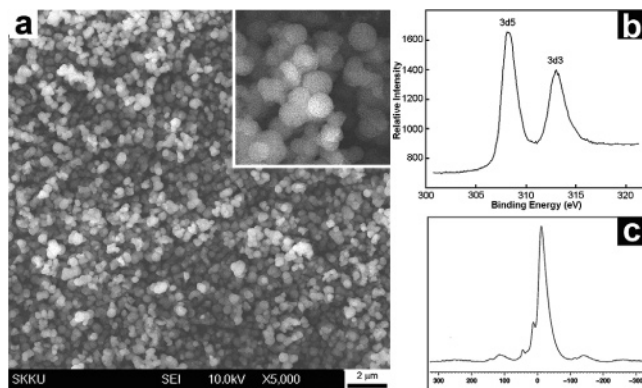


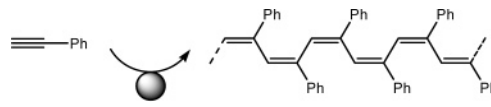
Figure 2. (a) FE-SEM image, (b) XPS of Rh 3d orbital, and (c) solid <sup>27</sup>Al NMR spectra of organometallic nanocatalyst, **ON3**.

The **ON** particles were investigated for catalytic activity in the polymerization of phenylacetylene. Poly(phenylacetylene) (PPA) has attracted considerable attention due to a range of potentially useful properties: photo and electrical conductivity, photoluminescence (PL), magnetism, liquid crystallinity, gas and liquid permselectivity, and third-order nonlinear optics. PPA can exist as two stereoisomers: cis-transoid (cis-PPA), trans-transoid (trans-PPA) forms.<sup>10</sup> cis-PPA has an interesting helical structure in solid-state, and its isomerization mechanism to trans-PPA has been intensively studied. Moreover, cis-PPA has been suggested as a spintronic material candidate for application in memory devices.<sup>11</sup> Thus, the stereoselective synthesis of PPA is desirable and necessary for device applications of these materials.

It has been reported that cis- and trans-PPA can be prepared with Rh-, Ir-, and Ni-based homogeneous organometallic catalysts.<sup>12</sup> Table 1 gives a summary of the catalytic activity of nanocatalysts **ON** in the polymerization of phenylacetylene. It is important to note that the Rh center in  $\text{I}^+$  undergoes a large change upon reaction

<sup>†</sup> Sungkyunkwan University.

<sup>‡</sup> Brown University.

**Table 1.** Polymerization of Phenylacetylene Catalyzed by ONs<sup>a</sup>


entry	catalyst	solvent	M <sub>n</sub>	M <sub>w</sub> /M <sub>n</sub>	yield (%) <sup>b</sup>
1	<b>1<sup>+</sup></b>	CH <sub>2</sub> Cl <sub>2</sub>	2900	1.8	90 (59)
2	<b>ON1</b>	CH <sub>2</sub> Cl <sub>2</sub>	4100	4.3	82 (86)
3	<b>ON2</b>	CH <sub>2</sub> Cl <sub>2</sub>	13 200	3.4	84 (94)
4	<b>ON2–Al</b>	CH <sub>2</sub> Cl <sub>2</sub>	12 900	2.3	81 (94)
5	<b>ON3</b>	CH <sub>2</sub> Cl <sub>2</sub>	15 600	3.5	86 (96)
6	<b>1<sup>+</sup></b>	THF	17 800	2.4	98 (59)
7	<b>ON1</b>	THF	23 600	1.8	88 (95)
8	<b>ON1</b>	THF	8800	2.9	67 (94)
9 <sup>c</sup>	<b>ON1</b>	THF	4100	4.3	54 (90)
10 <sup>d</sup>	<b>ON2</b>	THF	26 800	2.2	98 (95)
11 <sup>e</sup>	<b>ON2–Al</b>	THF	21 600	2.0	91 (96)
12	<b>ON3</b>	THF	29 200	2.2	98 (96)

<sup>a</sup> Conditions: 2.5 mL solvent, 1.2 mol % (19 mg) ON, 4.55 mmol PA, 18 h, rt. <sup>b</sup> Isolated yields; cis-PPA contents in parentheses. <sup>c</sup> 10 mL THF was used. <sup>d</sup> 20 mL THF was used. <sup>e</sup> 21 mg ON was used.

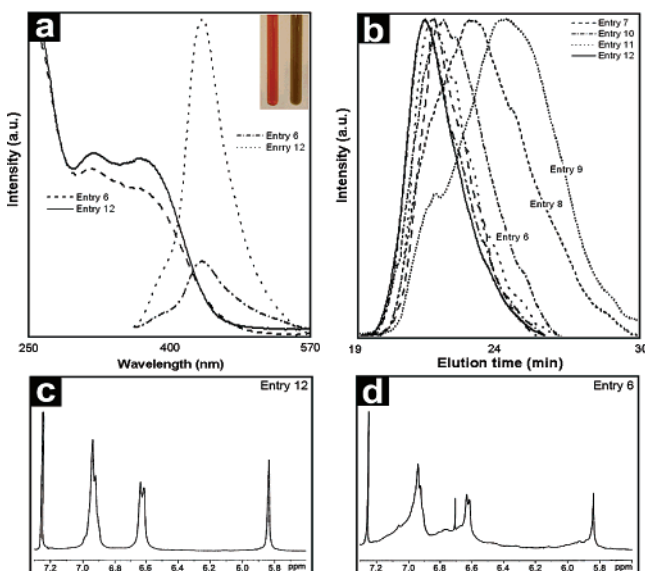


**Figure 3.** (a) UV–vis and emission spectra (CDCl<sub>3</sub>) of PPAs from entries 6 and 12 and (inset) photos of PPAs from entries 6 (right) and 12 (left), (b) GPC chromatograms of PPAs from entries 6–12 in Table 1, and (c,d) <sup>1</sup>H NMR spectra of PPAs from entries 6 and 12 in CDCl<sub>3</sub>.

with Al(Oi-Pr)<sub>3</sub> to generate the heterogeneous ON catalysts. During the self-supporting process, deprotonation of the –OH groups occurs and the η<sup>6</sup>-hydroquinone is converted to a η<sup>4</sup>-quinone ligand. The Rh acts as an electron sink in this conversion and undergoes a formal change in charge from +1 to –1.<sup>7a</sup>

As shown in Table 1, the ON catalysts produced much longer PPAs than did 1<sup>+</sup> (entry 1 vs 2–5, entry 6 vs 7 and 10–12). Moreover, the ONs were much more stereoselective (up to 96% formation of cis-PPA), while catalyst 1<sup>+</sup> produced a mixture of cis- and trans-PPA (59:41; Figure 3d).<sup>13</sup> The polymerization in THF gave longer and more narrowly distributed PPA with higher yields than in CH<sub>2</sub>Cl<sub>2</sub>. Figure 3b shows gel permeation chromatography chromatograms of the PPAs. As the size of ON was decreased, longer PPAs were obtained as a result of increased catalytic activity. As the solvent volume increased, the PPA lengths decreased dramatically, consistent with the heterogeneous nature of the reaction (entries 7–9) Catalyst ON3, recovered (19 mg) from the

reaction mixture by centrifugation after entry 12, gave a 94% yield in a second run (see Figure S3 in SI for a SEM image of recovered ON3).

PPA has a conjugated backbone that bodes well for useful photoluminescent materials. Figure 3a displays the UV–vis and PL spectra. Interestingly, the colors of PPAs obtained from ON3 and 1<sup>+</sup> are different (Figure 3a): bright red (from ON3) and dark yellow (from 1<sup>+</sup>). The PPA of entry 12 showed a stronger and sharper emission peak at 450 nm (380 nm excitation) than that of entry 6.

In conclusion, heterogeneous self-supported ONs were synthesized by treatment of the π-hydroquinone rhodium complex 1<sup>+</sup> with Al(Oi-Pr)<sub>3</sub>. The synthesis is triggered by deprotonation of the –OH groups by Al(Oi-Pr)<sub>3</sub>, with concomitant coordination of the quinone oxygen atoms to the aluminum and a η<sup>6</sup> to η<sup>4</sup> hapticity change in the bonding of the quinonoid ring to the rhodium. The organometallic nanocatalysts, the size of which can be controlled by alteration of the reaction conditions, show high catalytic activities in the stereoselective polymerization of phenylacetylene to produce cis-poly(phenylacetylene). The stereoselective nature of the catalysis is a property that evolves during the heterogenization process.

**Acknowledgment.** This work was supported by the Korea Research Foundation Grant funded by the Korean Government (MOEHRD; KRF-2005-005-J11901) and through a Faculty Research Fund-2005 funded by Sungkyunkwan University. We thank Mr. J. S. Ju at Cooperative Center for Research Facilities at Sungkyunkwan University for SEM study. D.A.S. acknowledges the National Science Foundation and the Petroleum Research Fund.

**Supporting Information Available:** Experimental details, size distributions of ONs, SEM images of ON3 before and after use, <sup>1</sup>H NMR of all PPAs, and XPS peak of Al 2p. This material is available free of charge via the Internet at <http://pubs.acs.org>.

## References

- (1) Astruc, D.; Lu, F.; Aranzas, J. R. *Angew. Chem., Int. Ed.* **2005**, *44*, 7852.
- (2) Gladysz, J. *Chem. Rev.* **2002**, *102*, 3215.
- (3) (a) Song, C. E. *Chem. Commun.* **2004**, 1033. (b) Dupont, J.; de Souza, R. F.; Suarez, P. A. Z. *Chem. Rev.* **2002**, *102*, 3667.
- (4) (a) Wang, X.; Ding, K. *J. Am. Chem. Soc.* **2004**, *126*, 10524. (b) Liang, Y.; Jing, Q.; Li, X.; Shi, L.; Ding, K. *J. Am. Chem. Soc.* **2005**, *127*, 7694.
- (5) *Applied Homogeneous Catalysis with Organometallic Compounds*; Cornils, B., Herrmann, W. A., Eds.; Vols. 1 and 2; Wiley-VCH: Weinheim, 1996.
- (6) Oh, M.; Mirkin, C. A. *Nature* **2005**, *438*, 651.
- (7) (a) Son, S. U.; Reingold, J. A.; Carpenter, G. B.; Sweigart, D. A. *Angew. Chem., Int. Ed.* **2005**, *44*, 7710. (b) Son, S. U.; Reingold, J. A.; Sweigart, D. A. *Chem. Commun.* **2006**, 708. (c) Son, S. U.; Kim, S. B.; Reingold, J. A.; Carpenter, G. B.; Sweigart, D. A. *J. Am. Chem. Soc.* **2005**, *127*, 12238.
- (8) The observed values of Rh 3d are between that of metallic Rh (307 eV) and that of Rh(I) (309 eV). The binding energies of Al 2p orbital in Al, Al<sub>2</sub>O, or AlO, and Al<sub>2</sub>O<sub>3</sub> are known as 73.0, 74.5, and 75.4 eV, respectively. Shin, E. W.; Han, J. S.; Jang, M.; Min, S.-H.; Park, J. K.; Rowell, R. M. *Environ. Sci. Technol.* **2004**, *38*, 912.
- (9) Aoyama, Y.; Dewa, T. *J. Mol. Catal. A: Chem.* **2000**, *152*, 257.
- (10) Percec, V.; Rudick, J. G.; Nombel, P.; Buchowicz, W. *J. Polym. Sci., Part A: Polym. Chem.* **2002**, *40*, 3212 and references therein.
- (11) Tabata, M.; Watanabe, Y.; Muto, S. *Macromol. Chem. Phys.* **2004**, *205*, 1174.
- (12) (a) Kishimoto, Y.; Eckerle, P.; Miyatake, T.; Ikariya, T.; Noyori, R. *J. Am. Chem. Soc.* **1994**, *116*, 12131. (b) Marigo, M.; Millos, D.; Marsich, N.; Farnetti, E. *J. Mol. Catal. A: Chem.* **2003**, *206*, 319. (c) Douglas, W. E. *Appl. Organomet. Chem.* **2001**, *15*, 23.
- (13) The peak at 5.84 ppm is due to a cis proton, while the peak at 6.78 ppm to a trans proton (see Supporting Information for <sup>1</sup>H NMR of all PPAs). Sun, J. Z.; Chen, H. Z.; Xu, R. S.; Wang, M.; Lam, J. W. Y.; Tang, B. Z. *Chem. Commun.* **2002**, 1222.

JA062907O